Present and Future of Modeling Global Environmental Change: Toward Integrated Modeling, Eds., T. Matsuno and H. Kida, pp. 29–48.

Toward a Unified Highly Resolved Regional Climate Modeling System

Yuqing WANG and Bin WANG

International Pacific Research Center, School of Ocean and Earth Science and Technology, University of Hawaii, Honolulu, HI 96822, U.S.A.

Abstract—Efforts have been made at the International Pacific Research Center (IPRC) to develop a highly resolved regional climate model, aiming at simulating variability of Asian-Australian monsoon system and assessing impacts of the global change on the Asian-Pacific climate. The overall goal is to realistically simulate regional and meso-scale features of the Asian-Australian monsoon system and associated hydrological cycle. To achieve this goal, the model should be highly resolvable for a wide range of transient disturbances such as tropical storms and mesoscale vortices in the Meiyu/Baiu front.

This paper discusses strategies for developing such a model based on a triply nested movable mesh primitive equation model that uses a two-way interactive nesting approach and an explicit cloud microphysics scheme. Our preliminary results suggest that for models with a resolution on an order of 10 km, the explicit mixed ice-phase cloud microphysics scheme has a superior physical basis and is less scale-dependent than implicit parameterization schemes such as deep, shallow convective parameterization currently being widely used in weather forecast and climate models. Especially, the better simulated downdrafts associated with organized convective systems by the explicit scheme can improve the simulation of meso-scale convective rain bands in severe storms or rain belts in Meiyu/Baiu fronts. The improved simulation of clouds (both spatial distribution and temporal evolution, and both water clouds and ice clouds) may provide physically based parameterization of cloud optical properties and fractional cloud amount and thus may potentially improve radiation budget and the cloud-radiation forcing in the climate models.

INTRODUCTION

Two research themes at the International Pacific Research Center (IPRC), the Asian-Australian monsoon system and the impact of global change on the Asian-Pacific regional climate, require conscientious modeling efforts using a highly resolved regional climate modeling system. We are now at the stage to develop our own regional climate model that is expected to be highly resolvable and to be able to realistically simulate both the large-scale features of the Asian-Australian monsoon system and its hydrological cycle, and meso-scale phenomena, such as tropical cyclones, Meiyu fronts and associated meso-vortices or rainbands within the monsoon system. The Asian-Australian monsoon involves multiscale motions

and their complex interactions. Process studies are crucial for improving our understanding of different physical mechanisms and scale interactions involved in the onset and evolution of the Asian-Australian monsoon system. In this regard, the regional climate modeling system to be built must have the capability of resolving multi-scale interactions.

The Asian-Pacific monsoon has many unique features. For instance, the Meiyu/Baiu is known for its narrow meridional scale and organized meso-scale convective systems, which differ from those seen in the other regions of the world (Ding, 1993; Chen *et al*., 1998). To realistically simulate the Meiyu/Baiu system poses a great challenge for existing climate models (Kang, 1999). Simulation of monsoon circulation with global general circulation models (GCMs) was found to be very sensitive to different cumulus parameterization schemes (Zhang, 1994). Limited modeling studies with regional climate models also indicated that some cumulus parameterization schemes do not seem to work well in the East Asian monsoon region (Wang, 2000). The western Pacific monsoon involves heavy activity of tropical storms; the collective effects of these transient storms have considerable contribution to the monthly and seasonal mean climate. Scale interactions are extremely complex in the Asia-Pacific monsoon region (Holland, 1995), which are further complicated due to the effects of Tibetan plateau, land surface processes, ocean-continent contrast, and air-sea interaction associated with storms. These specific features require special consideration in designing numerical models to be used in this particular region.

As a regional climate model, in addition to realistic simulation of regional climatology and seasonal mean climate anomalies, the model is required to be able to simulate climate scenarios in fine scales and the frequency of occurrence of severe weather events (such as tropical storms, torrential rainfall etc.). In order to improve the simulation and understanding of monsoon hydrological cycle, there is an urgent need to simulate precipitation on fine resolutions. These specific needs challenge the physical basis or validity of the hypotheses for usage of cumulus parameterization schemes in a numerical model, because at very high resolutions organized convection is no longer sub-grid phenomena (Molinari and Dudeck, 1992). In this regard, cumulus parameterization should be bypassed and explicit simulation of cumulus convection becomes necessary.

Our overall goal is to develop a highly resolved regional climate model that will be imbedded within a global coupled Atmosphere-Ocean-Land model, serving as a primary tool for climate process studies and predictability studies for the Asian-Australian monsoon system. For this purpose, we are working towards a unified regional climate modeling system in which cloud microphysics is treated explicitly and is allowed to interact with radiative processes, and a multiply nested movable mesh with two-way interaction is used to include the multi-scale interactions.

In order to model severe storms and multi-scale interactions in the Asian-Australian monsoon system, the use of explicit cloud microphysics scheme has its advantages. We argue that, for models with a resolution on an order of 10 km, the explicit cloud microphysics scheme has better physical basis and is less scale-

dependent compared to other cumulus parameterization schemes. This makes it appealing to establish a unified regional modeling system. Secondly, the Asian monsoon hosts variety of convective systems ranging from tropical storms, subtropical frontal systems, and moist baroclinic waves. The explicit scheme is potentially more suitable for simulating a wide range of weather systems. In particular, at high resolutions (e.g., less than 10 km), the explicit scheme has the capability of realistically modeling downdrafts associated with precipitation, organized meso-beta scale convective rain band and cloud properties. Detailed cloud microphysics can provide more realistic cloud information (cloud amount, cloud optical properties etc.) needed for radiation budgets and thus improve our understanding of cloud-radiation forcing in a large range of both spatial and time scales.

We will briefly describe, in Section 2, the numerical and physical aspects of the numerical model that we have chosen for further development, and present, in Section 3, some preliminary results from simulations of tropical cyclones and the intertropical convergence zone (ITCZ), which demonstrate the potential of the model and the importance of using explicit cloud microphysics in modeling tropical storms, long-term simulation of the ITCZ, and some low clouds (stratus) over the cold ocean in the winter hemisphere. The last section presents a summary and discusses the implications of the present work to the development of a global meso-scale model using the Earth Simulator.

THE NUMERICAL MODEL

The numerical model to be implemented is a triply nested movable mesh, high-resolution mesoscale model newly developed by Wang (1999). A detailed description of the numerical model and its performance and capability of simulating scale interactions in tropical cyclones can be found in Wang (1999, 2001a, b, c). For brievity, only some key features of the numerical model will be discribed. The current version of the model uses hydrostatic primitive equations formulated on spherical longitude/latitude grids with sigma (pressure normalized by the surface pressure) as the vertical coordinate. To facilitate long-term integration, the model uses a second-order conservative finite-difference scheme on an unstagered grid system (Arakawa A grid) and a second order leapfrog scheme with intermittent use of Euler backward scheme for time integration. The model has 20 (flexible) levels in the vertical with substantial concentration of resolution (at least five levels) within the planetary boundary layer.

The model domain is (optionally) triply nested with the two interior meshes being movable so that the interested weather systems (such as tropical storms or severe weather systems) can be always located near their centers. To include the multi-scale interactions between the interested weather system and its environment, a two-way interactive nesting is used in such a way that the coarser mesh first provides the lateral boundary condition to the finer mesh, while the results from the fine mesh integration then feeds back to the coarse mesh. In this two-way nesting system, all the meshes should proceed simultaneously to ensure the feedback occurred at the same time levels. The grid-spacing and time-step ratio

is 9:3:1. The outermost and intermediate meshes are used to represent large-scale circulation and synoptic scale flows and the innermost mesh resolves the core region and rainbands of severe weather systems.

The model physics are carefully chosen based on the up-to-date developments. The subgrid-scale vertical mixing is accomplished by a 1.5-order turbulence closure scheme in which both the turbulent kinetic energy and its dissipation rate are prognostic variables (Detering and Etling, 1985). In our implementation, we have included both advection process and the effect of the moist-adiabatic processes in cloudy air on the buoyancy production of turbulence (Durran and Klemp, 1982). Turbulent fluxes at the surface are calculated using a modified Monin-Obukhov scheme-the TOGA CORE algorithm (Fairall *et al*., 1996). Effects of sea spray evaporation (Fairall *et al*., 1994; Andreas and DeCosmo, 1999) and dissipative heating (Bister and Emanuel, 1998) are both considered as options by special experimental design.

The parameterization of cloud microphysics is based on the existing schemes that are extensively used in cloud and meso-scale models in recent years (Lin *et al*., 1983, Rutledge and Hobbs, 1983, 1984; Reisner *et al*., 1998). Prognostic variables in this scheme include mixing ratios of water vapor, cloud water, rainwater, cloud ice, snow and graupel. Cloud water is assumed to be monodispersed and to move with the air, while cloud ice is monodispersed but precipitates with the terminal velocity given by Heymsfield and Donner (1990). Condensation/evaporation of cloud water takes place instantaneously when the air is supersaturated/subsaturated. There are 36 different cloud microphysical processes that are considered in our explicit cloud microphysics scheme (see Wang, 1999, 2001a for details).

To facilitate climate research and realistically simulate the cloud-radiation feedback, the radiation scheme allows interactions between the atmosphere, cloud and precipitation fields and the surface. Three options are available in the model although further parameter-tuning and validation are required. They are simple diagnostic cloud scheme used in the Florida State University global model (Krishnamurti *et al*., 1990); the simple prognostic cloud scheme used as an option in the fifth-generation Penn State University/NCAR mesoscale model (MM5) (Dudhia, 1989); and a fully coupled complicated and accurate radiation package developed by Edwards and Slingo (1996) and further modified recently by Sun and Rikus (1999). Details of these radiation schemes used in the model can be found in the references cited above.

SOME NUMERICAL RESULTS

Simulation of tropical cyclones

To obtain realistic structure and intensity of a tropical cyclone, the numerical model should resolve meso-beta scale convective systems in both the inner core region and the outer spiral rainbands. In this regard, a 5 km grid size is necessary and use of an explicit cloud microphysics scheme is feasible since organized convection can be well resolved at this resolution. On the other hand, a mixed ice-

phase cloud microphysics scheme is required to realistically simulate the downdrafts associated with meso-scale convective systems that may in turn affect the organization of convection in both the core region and rainbands. To illustrate the striking performance of the numerical model introduced in the last section in simulating tropical cyclones, some results from a one-week simulation of a tropical cyclone are presented. To save computational time, the radiation has not been included in the tropical cyclone simulation.

In a control experiment, in which a uniform SST of 29°C was specified as a lower boundary condition, an initial vortex with 25 m/s maximum tangential wind was imbedded into a resting environment on an *f*-plane of 18°S. The tropical cyclone intensified rapidly from 12 to 62 h, and then experienced a dramatic intensity change between 62 and 90 h, and then reached a quasi-steady state, which is accompanied by a moderate oscillation in intensity (Fig. 1). The tropical cyclone reached its maximum intensity with a minimum central pressure of 903 hPa and a maximum wind speed of 66 m/s. A fluctuation in the maximum wind speed before 24 h was due to the development of squall-type convection and associated outward propagating gravity waves (Wang, 2001a). The intensity change between 62 and 90 h is remarkable and interesting, and was caused by a unique structure change including a breakdown and recovery cycle of the eyewall (Wang, 2001b, c).

The overall symmetric structure of the simulated tropical cyclone at mature stage can be seen from Fig. 2. The maximum tangential wind is located at a radius of about 30 km in the boundary layer about 300 m from the sea surface (Fig. 2a). Strong inflow occurs in the boundary layer just outside of the maximum tangential

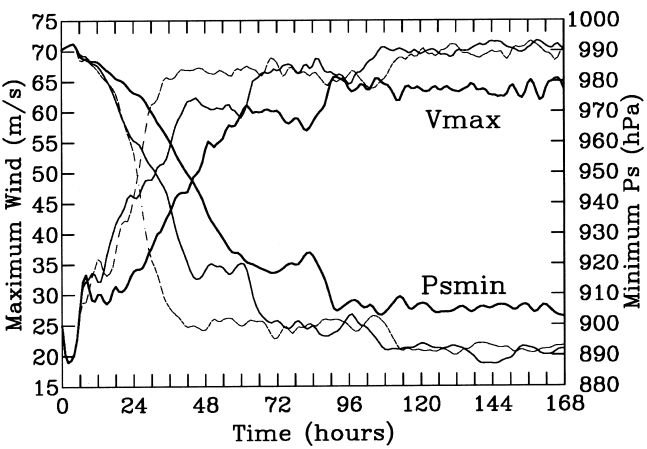

Fig. 1. The minimum sea surface pressure (a) and maximum wind speed about 20 m above sea surface (b) as a function of time for the simulated tropical cyclones in three experiments: a control one with mixed-ice phase cloud microphysics scheme (thick solid); warm-rain process only cloud microphysics scheme (immediately thick); and the one with a mixed ice-phase but without melting of snow and graupel and evaporation of rain (thin).

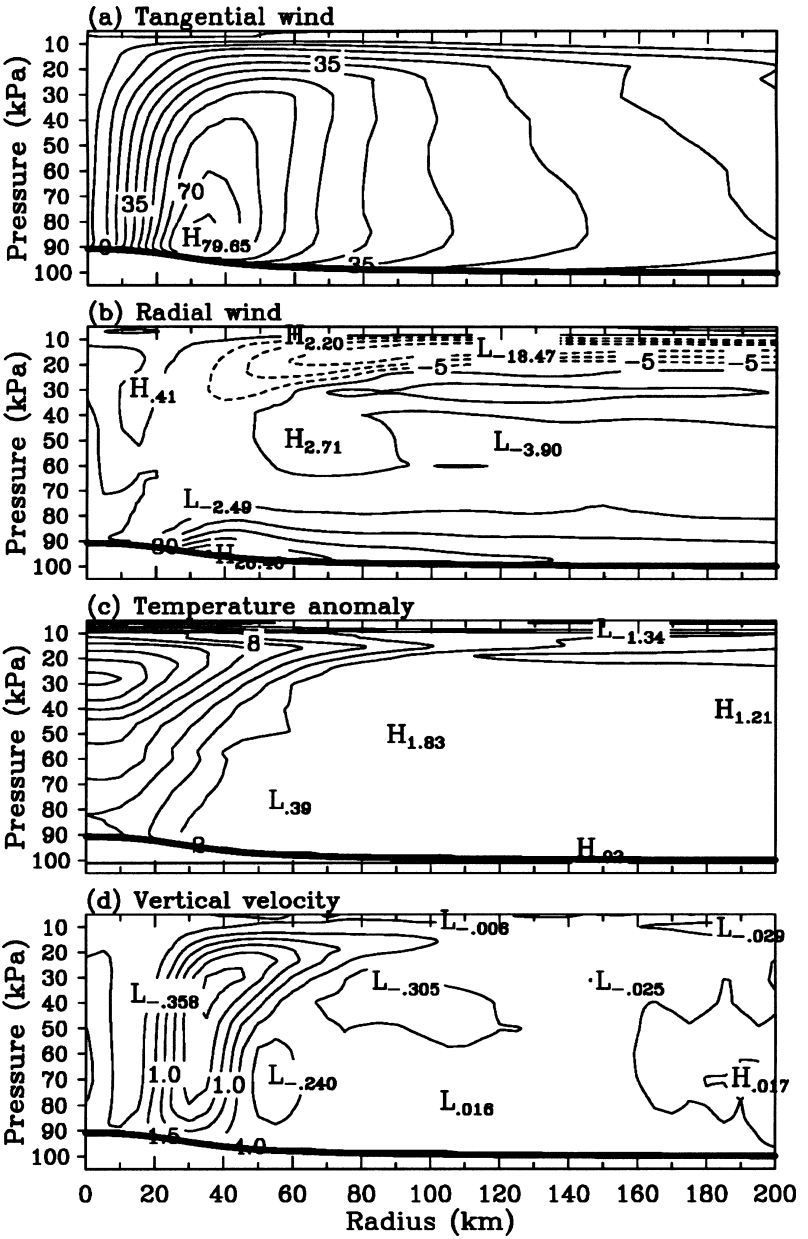

Fig. 2. The symmetric structure of the simulated tropical cyclone at the mature stage after 90 h simulation: (a) tangential wind (m/s), (b) radial wind (m/s), (c) temperature anomaly (K), and (d) vertical motion (m/s).

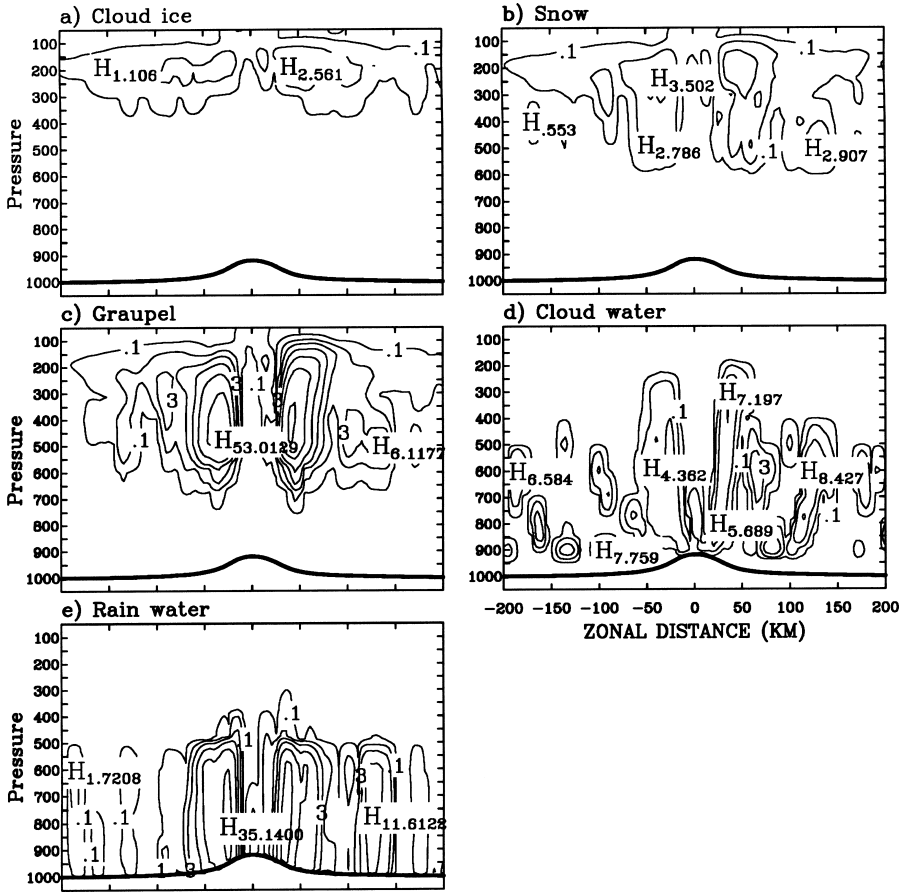

Fig. 3. A zonal-vertical section of all hydrometeors (10^{-4} kg/kg) crossing the simulated tropical cyclone center after 60 h of simulation.

wind with maximum inflow of about 25 m/s. There is a broad outflow layer located in the upper troposphere outside the eye wall (Fig. 2b). The cyclone has a warm core structure with a maximum temperature anomaly of 18°C at about 250–300 hPa (Fig. 2c). An upper-level warming extends to large radii due to diabatic heating in cirrus clouds. There is weak descending motion in the eye and strong updraft in the eye wall that tilts outward with height (Fig. 2d). All these features compare fairly with observed tropical cyclone structures (Frank, 1977). These realistic structures could not be well simulated if a coarse resolution was used (say, more than 15 km). This is the case because the coarse resolution cannot resolve the large gradients between the eye and the eyewall, only tens of kilometers from the center, in a tropical cyclone.

The model produces realistic distribution of cloud microphysical quantities,

such as the mixing ratios of cloud ice, snow, graupel, cloud water, and rainwater (Fig. 3). The cloud ice is concentrated in the upper troposphere with a maximum at 200 hPa in the eyewall region and extends radially outward (Fig. 3a). It is initiated through nucleation and freezing of supper-cooled cloud water and advected outward radially by the upper tropospheric outflow. Snow forms as the cloud ice grows to a critical mass (size) and concentrated in the layer between 200 and 400 hPa (Fig. 3b). Snow starts to convert to graupel as its size exceeds a critical value. Graupel also forms through freezing of rainwater and grows by collecting liquid and solid particles as it falls through the melting layer. Thus, the maximum graupel mixing ratio occurs just above the freezing level in the eyewall around 400–500 hPa (Fig. 3c). The cloud water comes from condensation of supersaturated water vapor; thus high concentration of cloud water is found in the tilting updraft in the eyewall (Fig. 3d). Rain (Fig. 3e) forms as conversion from cloud water and collection of cloud water, and evaporates when it falls through unsaturated air. Note that these cloud properties are input variables in radiation calculation and thus realistic distribution and quantity are very important because the cloud optical properties are very sensitive to cloud water/ice contents. Our preliminary tests with a coupled radiation scheme showed that the cloud water content in this simulation is too high and thus could give rise excessively thick water clouds. We have fixed this problem by reducing the critical mixing ratio for autoconversion of cloud water to rain water and by using a timely adjustment of condensation with other microphysical processes to replace a final adjustment used in the early version of the cloud microphysics scheme and used in MM5 as well (Reisner *et al*., 1998).

Figure 4 presents a plan view (a) of the model-estimated radar reflectivity at the surface simulated in the control experiment after 86 h 30 min and its vertical cross section (b) through line A–B in (a). The model produces realistic eye with very low reflectivity, eyewall with high reflectivity, and both the inner and outer spiral rainbands. The eyewall is encircled by high radar reflectivity with an opened shape to the northwest connected with an inner spiral convective rainband (Fig. 4a). There are some regions with relatively low reflectivity within the eye, indicating the existence of light precipitation there. Except for several small inner spiral rainbands just outside the eyewall, there are two primary spiral rainbands between 80 and 180 km from the cyclone center (Fig. 4a). The high radar reflectivity in the eyewall tilts outward with height and is located below the melting level at about 500 hPa in the eyewall (Fig. 4b). Just outside the eyewall, low radar reflectivity is related to stratiform precipitation in the mid-upper troposphere or shallow convection in the boundary layer, and high reflectivity is related to deep convection in the convective rainbands (Fig. 4b). Relatively low reflectivity in the eye accompanied by light precipitation seen in Fig. 4a extends to a level up to about 700 hPa, sometimes above 500 hPa (Fig. 4b), a feature usually observed in strong tropical cyclones.

One of the factors that might considerably impact the intensity of the tropical cyclone is the downdrafts near the eyewall environment. The downdrafts associated with deep convection or stratiform precipitation can play a role in bringing the dry

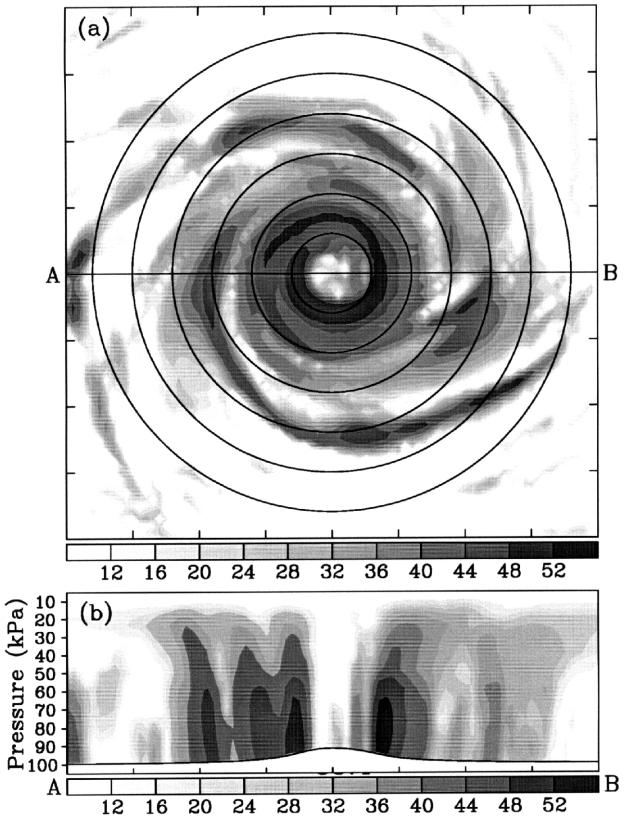

Fig. 4. Horizontal plan view of (a) the simulated radar reflectivity (in dBZ) at the surface in the tropical cyclone inner region (400 km by 400 km) and its zonal vertical cross-section (b) along the line A–B in (a).

and cold air with low equivalent potential vorticity from the midtroposphere to the planetary boundary layer where they may be advected toward the core region and entrained into the eyewall. Once such a process happens, the eyewall convection could be somewhat suppressed. This may be one of the factors that limits the tropical cyclone intensity in nature. Therefore, to realistically simulate the intensity of tropical cyclones the model should be able to explicitly resolve these downdrafts. Except for the high model resolution, choosing suitable cloud microphysics scheme is also critical. Our numerical results have already shown that a mixed-ice phase cloud microphysics scheme is necessary in this regard. To illustrate this statement, we included also in Fig. 1 the evolution of the tropical cyclone intensity from another two experiments. In one of the experiments, we considered only the warm rain processes, while in the other, we excluded the cooling effect due to both melting of snow and graupel, and the evaporation of rain. We can see that not only the intensification rate is strikingly larger but also

the final intensity of the simulated tropical cyclone is stronger in the two supplementary experiments than those in the control experiment. In the experiment with only the warm rain processes, the evaporation of rain was allowed and thus some weak downdrafts were present in the simulation although they were quite weaker than those in the control experiment. However, in another experiment, although a mixed-ice phase cloud microphysics scheme was used, both melting of snow and graupel and the evaporation of rain were excluded. Therefore the major mechanism that initiates downdrafts in the model was totally missing. As a result, the intensification rate in this experiment was largest although the final intensity was similar to the one in the experiment with only the warm rain processes due to the fact that during the mature stage the boundary layer becomes nearly saturated in the near core region and thus the evaporation of rain became insignificant.

Simulation of the landfalling tropical cyclone is another test of the model's capability in dealing with storm interaction with land surface processes. The land surface condition (topography, roughness, temperature, wetness etc.) may directly influence tropical cyclones by increasing surface friction and decreasing evaporation once the storm moves across the coast. It may also indirectly affect the storm through modifying large-scale environmental flows. In general, the destructive effects of the land processes would weaken landfalling storms. However, recent observations revealed that some storms temporarily intensify when approaching a coast. An example is the Hurricane Andrew 1992 in Miami. It initially weakened but then re-intensified when approaching the Florida coast. However, after it crossed Florida and the Gulf of Mexico and during the second landfall at Louisiana, it continuously weakened without temporal re-intensification. The temporal intensification before the center landing is not always observed. There must be some specific processes that are responsible for this intensity fluctuation during the landfall. These processes are most likely associated with the land surface condition and perhaps also associated with internal storm dynamics.

To test the sensitivity of the landfall behavior to land surface conditions, we have designed a set of experiments: a control experiment without land, a warm land experiment in which the land surface temperature is the same as SST, and a cold land experiment in which the land surface temperature is 2 K lower than the adjacent ocean. An axially symmetric vortex was initially imbedded in a uniform easterly flow of 5 m/s which steers the cyclone moving toward a landmass with a north-south oriented coast. In the warm land experiment, a fluctuation in intensity similar to the one that was observed for Hurricane Andrew 1992 was obtained, while it is failed to reproduce this intensity change in the experiment with a cold land. A detailed analysis indicates that in the warm land experiment, there was a major rainband formed on the landward side first, while further approaching the coast, storm weakened due to the developing rainband which blocked the inflow to the core region of the cyclone in the boundary layer. However, as the cyclone further approached the coast, the rainband also spiraled towards the core, this was followed by a primary eyewall collapse and a core

contraction and a temporal intensification of the storm. In the cold land experiments, however, there was no intense rainband formed on the landward side, and thus the eyewall contraction and the intensification before landfalling were absent.

The difference between warm and cold land simulations is related to the land surface conditions. When land is warm, the surface heat fluxes and convective instability in the boundary layer are favored, which partially offset the effects of increased frictional dissipation and reduced evaporation. The Ekman convergence increases near the coast due to the change of roughness from ocean to land, which can contribute to the initiation and development of the rainbands on the landward side and the temporal intensification before the storm makes landfall. The cold land surface, on the other hand, makes the surface layer stable and decoupled with the upper boundary layer. Such a decoupling cuts off the latent heat supply dramatically, reduces the near coastline convergence associated with change of the friction across the coast, and thus is not favorable to intensification at pre-landfall. Detailed studies to examine the effects of wetness of land on the landfalling tropical storms and to determine the precise processes through which the land processes affect landfalling tropical cyclones are our future subject. It is worthwhile to point out that a repeated warm land experiment with a mass flux cumulus parameterization scheme with a resolution of 18 km, the model failed to reproduce the pre-landing reintensification. This suggests that use of high-resolution model to resolve the inner core structure of the storm and the initiation and development of near core rainbands holds a key for the simulation of the intensity change of a tropical cyclone.

Simulation of the ITCZ in zonally-symmetric two-dimensions

A 2D (zonally-symmetric two-dimensional) simulation of the ITCZ with a resolution of 0.25 degree latitudes is performed. The purposes are to test the model's capability for long-term integration and to investigate some issues associated with Hadley circulation and the annual cycle of the ITCZ. There are three questions with which we are concerned. First, the positions of the ITCZ simulated in numerical models are known to be sensitive to different cumulus parameterization schemes (e.g., Numaguti and Hayashi, 1991; Hess *et al.*, 1993). What will happen in a model with explicit cloud microphysics? Secondly, the Hadley circulation induced by an imposed off-equatorial heating is much stronger than that induced by an equatorial heating (e.g., Lindzen and Hou, 1988). Does this remain valid for an interactive heating and does the feedback between the heating and circulation further enhance the convection in off-equatorial ITCZs? Finally, why does the ITCZ in the eastern hemisphere display a sudden jump in the transitional season even though the seasonal migration of the maximum SST is gradual?

To address these questions, we have performed three experiments. The first two experiments examine steady responses of the atmosphere to a given SST distribution (symmetric and asymmetric about the equator, respectively), while in the third experiment we inspect the annual march of the ITCZ for given annual cycle SST forcing. In these experiments, the simple radiation scheme of Dudhia

(1989) was used with consideration of diurnal cycle. In the first two experiments with fixed SST forcing, we ignored the annual variation of the solar declination angle. Therefore, in the symmetric SST forcing an equinox condition was used while in the asymmetric SST forcing (with a maximum SST at 12°N for northern summer) the solar declination angle was set to be September 1 of an arbitrary year. In the third experiment with a seasonal migration of the SST forcing, the present day annual variation of the solar declination angle was included. The SST was specified as a function of latitude in the first two experiments, and of time in the third experiment according to

$$\mathrm{SST} = 273.16 + \Delta T \exp\left\{-4\left[\left(\varphi - \varphi_s\right) / L\right]^2\right\};$$

where φ is the latitude in degrees; $L = 90°$; $\Delta T = 29$ K. And φ_s is the latitude of the SST peak, which was set to 0 for symmetric forcing and 12°N for asymmetric forcing in the two fixed SST experiments, while it varies with time in the third experiment according to

$$\varphi_s = R \sin\left[2\pi\left(\mathrm{day} - 135\right) / 365\right]$$

where R (12° was used here) is the highest latitude in degrees that the peak SST can reach (at day = 135, Julian day of May 15).

When SST forcing was perfectly symmetric about the equator, the simulated rainfall distribution (solid curve in Fig. 5) shows enhanced convection near the equator. However, it is not exactly symmetric about the equator. This result differs from that obtained using Kuo (1974) and Arakawa-Schubert (1974) schemes, while bears resemblance to the result obtained using moist convective adjustment (MCA) scheme (Manabe *et al*., 1965) in the sense that both display a concentration of rainfall near the equator. The MCA scheme, however, yields a single maximum at the equator, whereas the explicit simulation results in a peak resided on the equator with an asymmetric distribution of rainfall about the equator. It should be pointed out that the over-equator convective maximum is an unstable mode in our 2D simulation. The rainfall shown in Fig. 5 is a time mean of the first 6 month simulation. Our results showed that the simulated ITCZ shifted across the equator with a period of about two days (not shown) although the maximum SST was maximum at the equator. Such an unstable nature results from interactions between the convection and circulation, and cloud-radiation forcing being included in the model.

When we force the model using the equatorially asymmetric SST, in which the maximum SST has the same amplitude as that in the equatorial symmetric forcing but it is located at 12°N, a single ITCZ is formed over the maximum SST. The maximum rate of precipitation is three times that in the equatorial symmetric SST case (dashed curve in Fig. 5). This indicates that an asymmetric distribution of SST favors a much stronger ITCZ. The interaction between the convection and

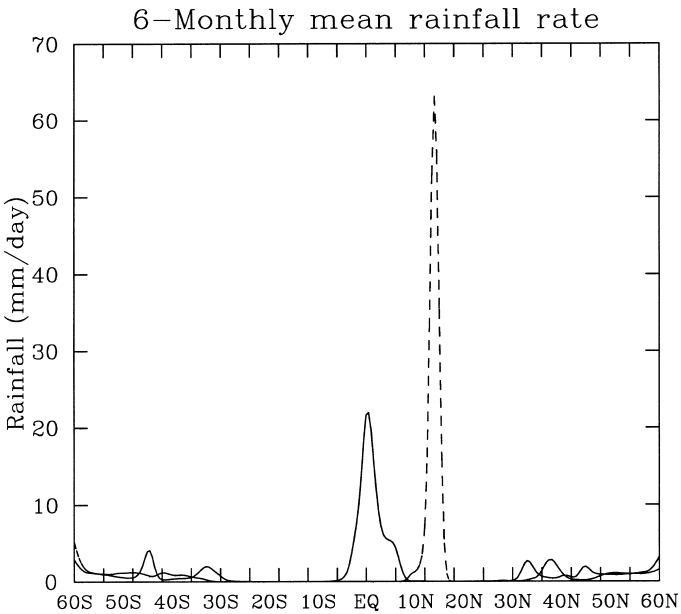

Fig. 5. A 6-monthly mean rainfall rate in the two experiments with fixed SST forcing in 2D model simulation of ITCZ. Solid is for equatorially symmetric SST forcing, while dashed for asymmetric SST forcing.

circulation (Waliser and Somerville, 1994), and also the cloud-radiation forcing (or convective-radiative feedback as discussed by Albrecht and Cox (1975) and by Raymond (2000) both enhance the equatorial asymmetry of the ITCZ.

To demonstrate the capability of the model in simulating both the cloud microphysics and interaction between clouds and radiation, and especially the low stratus clouds over the cold water (such as those observed over the south eastern Pacific), we show in Fig. 6 the monthly mean meridional-vertical cross section of temperature (a), mixing ratio of water vapor (b), zonal wind speed (c), meridional circulation (d), condensational heating rate (e) and radiational cooling rate (f). In agreement with Lindzen and Hou (1988), the temperature in the tropics is quite uniform above about 800 hPa and the westerly jet over the winter hemisphere is much stronger than that over the summer hemisphere (Fig. 6c), as well as the Hadley circulation (Fig. 6d). The winter hemisphere becomes very dry (Fig. 6b) and thus experiences enhanced longwave radiational cooling (Fig. 6f) as demonstrated by Raymond (2000). Condensational heating is concentrated in a very narrow latitude band a little north of the maximum SST (Fig. 6e). A striking feature that we should emphasize is that a large-scale condensational heating in the boundary layer extends from the equator southward to about 35°S (Fig. 6e). The condensational heating is responsible for the boundary layer stratus, which in term resulted in large net radiational cooling at its top (Fig. 6f). For the

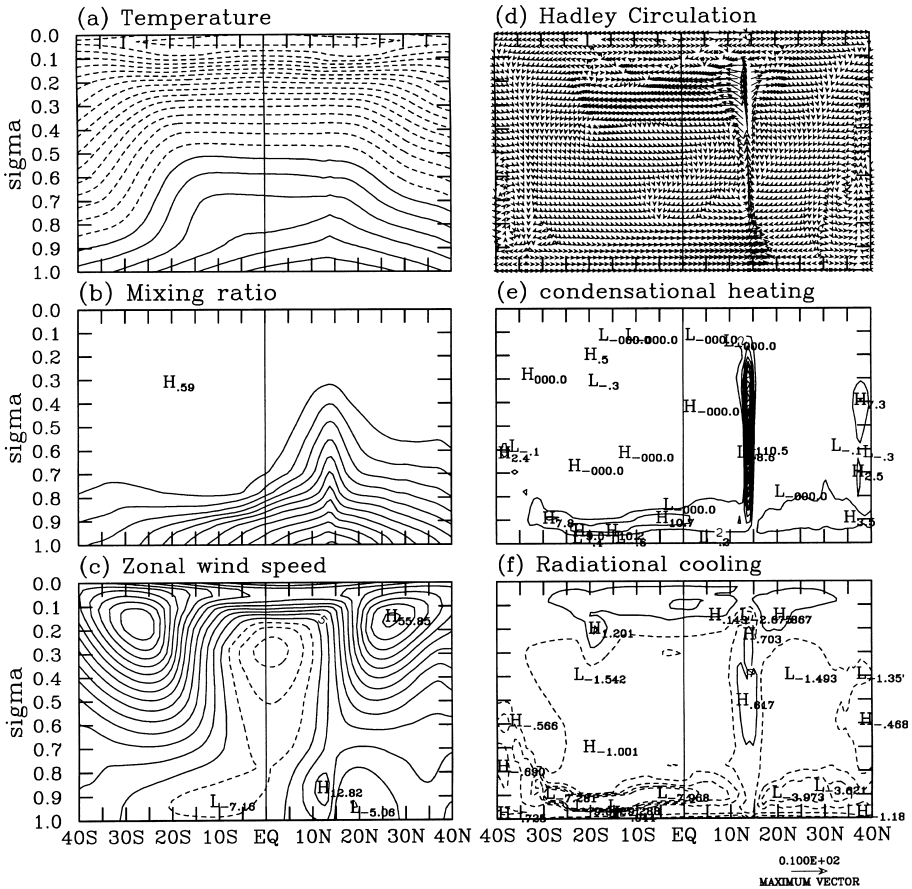

Fig. 6. Monthly mean meridional-vertical cross-section for the off-equator fixed SST forcing.

convective cloud within the ITCZ, a net radiative warming in the cloud and a net cooling at its top can be identified by comparing Fig. 6e with Fig. 6f. It is this differential heating (or cooling) that contributes to a much stronger off-equator ITCZ, the Hadley cell and the westerly jet in the ITCZ-free hemisphere. Realistic simulation of boundary layer clouds could not be obtained in most current GCMs or even in regional climate models that have been developed previously. Our successful simulation of the boundary layer clouds therefore is very encouraging.

In the experiment with a specified annual cycle of SST forcing, the model simulated annual mean zonal wind, meridional circulation, and temperature and mixing ratio all resemble closely to the observed counterparts (not shown). The annual mean precipitation shows a double ITCZ with maximum rainfall located at 10°N and 10°S, respectively (Fig. 7). This result differs fundamentally from the steady response to the corresponding annual mean SST forcing, suggesting that

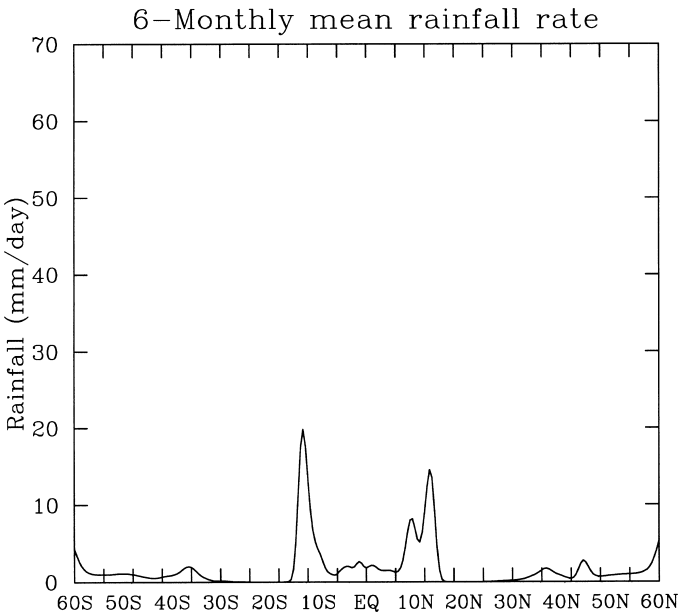

Fig. 7. Annual mean rainfall rate as a function of latitude in the experiment with an annual cycle SST forcing.

the annual variation of the convergence zone induced by the annual cycle SST forcing has a fundamental contribution to the formation of the time-mean ITCZ. We also noticed that the tropical easterly in the upper troposphere disappeared in the equatorially symmetric SST forcing, while it had a distribution and magnitude similar to the observations (not show), indicating that the annual cycle contributes to the annual mean considerably, especially in the tropics, as suggested by Wang and Wang (1999) in a simple coupled atmosphere-ocean model. The daily averaged surface winds and daily rainfall show a sudden seasonal transition between May and June, and between November and December although the SST forcing changes smoothly with season (Fig. 8). This sudden seasonal transition is favorably comparable with observations (Chao, 2000). The model, therefore, captures well the dynamics that determine seasonal jump of the ITCZ from one Hemisphere to another.

There are two sets of factors that contribute to the annual mean double ITCZ and the sudden seasonal transition. First, the atmospheric Ekman pumping associated with the high SST and low pressure is weak in the vicinity of the equator; even though the maximum SST shifts to the equator, the convection cannot develop strongly at the equator. This is possibly the reason why an equatorial heating produces weak upward motion and weak Hadley circulation. A more important factor is associated with the cloud-radiation feedback as discussed above. Suppose we start from the northern summer (see Fig. 8), the

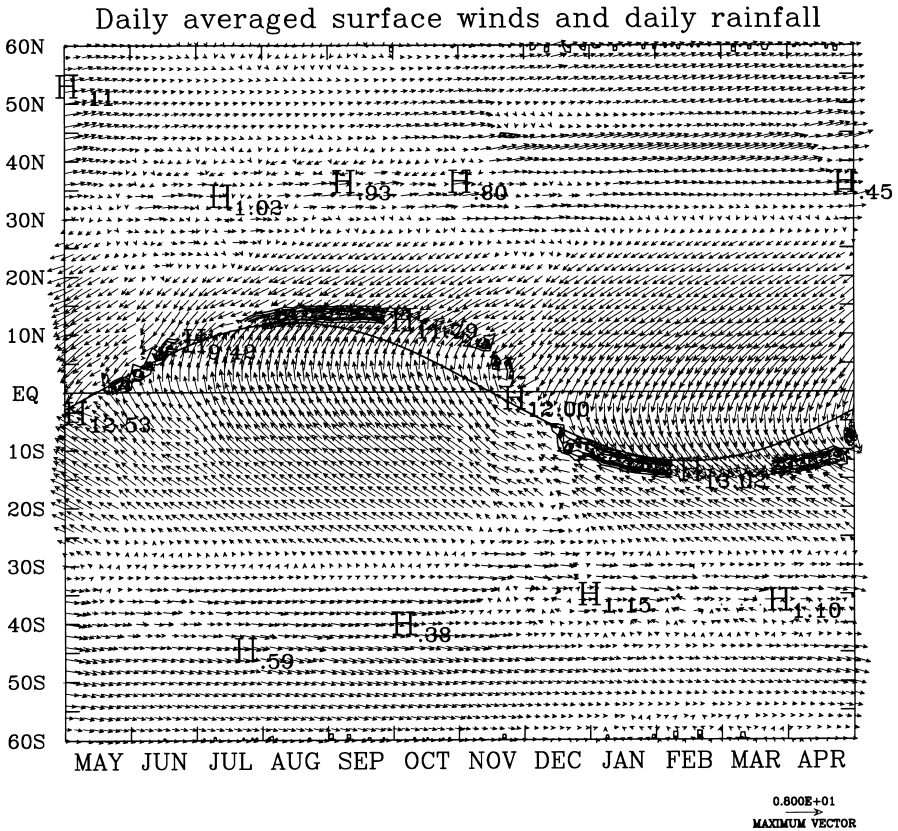

Fig. 8. Meridional-time distribution of daily averaged surface winds and daily rainfall in the experiment with an annual cycle SST forcing.

ITCZ is located north of the equator with a strong updraft and large amount of clouds and water vapor. This would result in a net radiational warming in the ITCZ zone. On the other hand, the air in the winter hemisphere is dry and the descending branch of the Hadley cell induces an inversion layer, thus the low stratus clouds forming beneath. As such, there is strong net radiational cooling above stratus clouds. This radiational cooling would increase surface pressure that would further enhance the low-level cross-equatorial flow toward northern convergence zone. The radiational cooling also requires a balance from adiabatic heating which is achieved by relatively strong descending motion, and thus a stronger Hadley circulation. Both positive feedbacks enhance the northern Hemisphere ITCZ and suppress convection over the equator. When the maximum SST shifts southward toward the equator, the southern winter Hadley circulation remains its dominance because the afore-mentioned positive cloud-radiation feedback tends to maintain the strength of the northern ITCZ. As a result, an

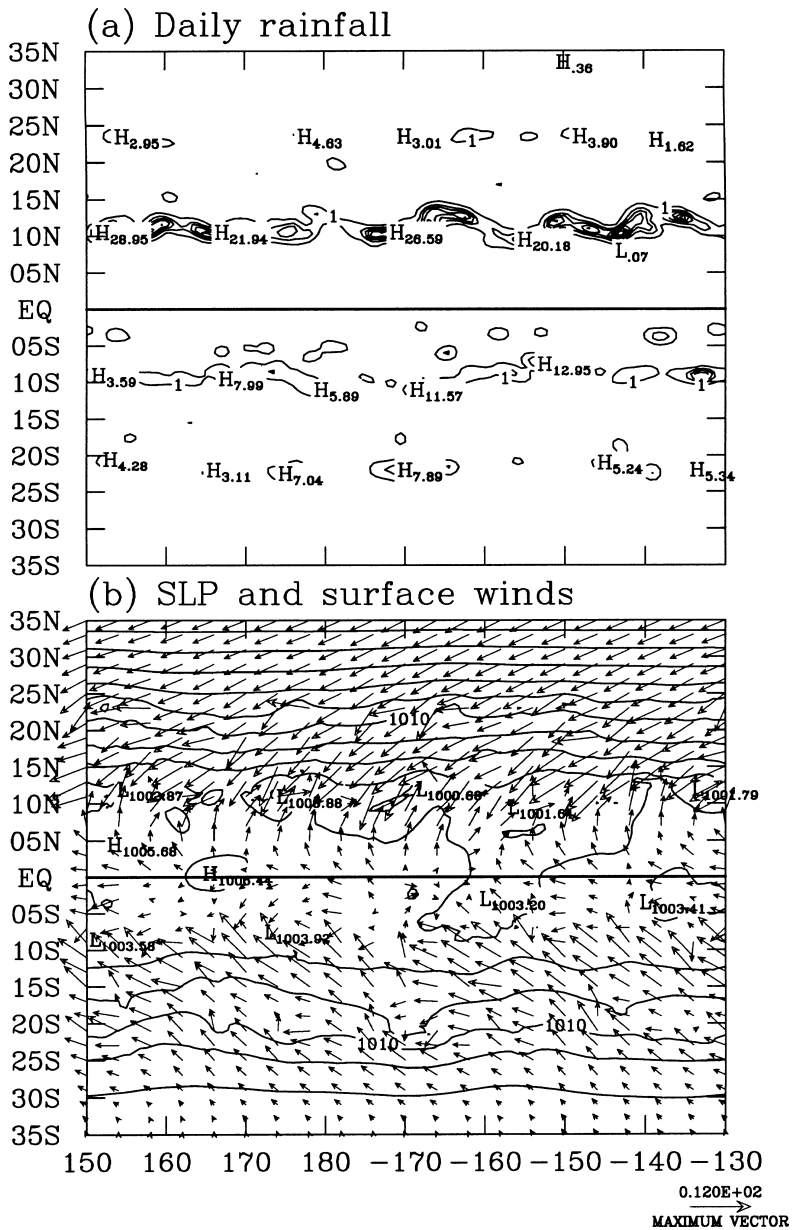

Fig. 9. Daily rainfall (a) and the sea level pressure and winds (b) in the 3D simulation with fixed summer SST observed over the central-eastern Pacific.

immediate shift of ITCZ following the movement of the maximum SST is prohibited, although the northern ITCZ itself weakens. Once the maximum SST crosses the equator, a southern ITCZ would quickly established because the inversion and stratus clouds are destroyed by the increased SST below, which destabilizes the boundary layer, and by the reduced descending motion above due to the weakening ITCZ in the Northern Hemisphere. Therefore, the movement of the convection zone from the Northern to Southern Hemisphere would be more like a "jump". The short residence time of the ITCZ over the equator leads to a bimodality of the locations of the convergence zone in the annual mean field.

Simulation of the ITCZ in three-dimensions

A 3D simulation with a resolution of 0.5 degree latitudes and with a fixed northern summer SST zonally averaged over the central-eastern Pacific shows a much stronger ITCZ in the Northern Hemisphere where the SST is higher than that in the Southern Hemisphere where a very weak ITCZ formed (Fig. 9). The formation of the double ITCZs is due to the fact that the SST over the equator is lower than the SST on each side of the equator. Unlike a zonally aligned convective rain belt obtained in the 2D simulations, the ITCZ in the 3D simulation exhibits transient behavior similar to that observed from satellite images. The disturbances developed in the ITCZ have wavelengths between 2000 km and 3000 km. These disturbances have contributed to both zonal mean and annual mean tropical circulation. It is also observed that in some cases, tropical cyclones could develop from these disturbances and result in a breakdown of the ITCZ (not shown). We found that cloud-radiation forcing plays significant role in the simulated pattern in both rainfall (Fig. 9a) and circulation fields (Fig. 9b). This 3D simulation demonstrates that even at a resolution as large as about 50 km, use of explicit cloud microphysics scheme can produce reasonable results.

SUMMARY

Our experiments demonstrated that explicit treatment of the cloud microphysics in regional numerical models yields promising simulation of realistic tropical storms and tropical convergence zones. In order to model the intensity of severe storms, use of a 5-km resolution is necessary because the inner core structure and evolution have to be adequately resolved in the model. On such a fine scale, the explicit treatment of the cloud microphysics is arguably better than cumulus parameterizations. We have also demonstrated that a conjunct use of the cloud microphysics scheme with a 1.5-order turbulence closure scheme is capable of realistically simulating mesoscale structure of the ITCZ with a model resolution as large as 50 km. This points to a possibility that explicit cloud microphysics scheme can widely used in the model with a wide range of resolution from a few kilometers to several tens of kilometers.

Although more tests are needed, we tentatively suggest that in a global mesoscale model, use of explicit cloud microphysics is feasible and may be of great value. Such an explicit treatment of clouds allows further increase the

model's resolution to an order of 1 km as long as the computer power is sufficient. A scale-independent scheme for mathematically description of cumulus convection is a logical target. The explicit scheme is arguably best suitable for a unified numerical model system for the Earth Simulator.

We plan to carry out a multi-suit of experiments to compare explicit scheme with other cumulus parameterization schemes in their simulation of variety of weather systems and, in particular, heavy rainfall events in the Asian-Pacific monsoon region. We also plan to implement a land surface model and coupled the regional atmospheric model with monsoon ocean models in the near future.

Acknowledgments—The first author is grateful to Dr. Shangping Xie for many helpful discussions and comments on the manuscript. This study has been supported in part by the US Office of Naval Research under grant ONR-00014-1-0493 and in part by the Frontier Research System for Global Change through the International Pacific Research Center in the School of Ocean and Earth Science and Technology at the University of Hawaii, Hawaii, USA.

REFERENCES

Albrecht, B. and S. K. Cox, 1975: The large-scale response of the tropical atmosphere to cloud modulated infrared heating. *J. Atmos. Sci*., **32**, 16–24.

Andreas, E. L. and J. DeCosmo, 1999: Sea spray production and influence on air-sea heat and moisture fluxes over the open ocean. In *Air-Sea Exchange: Physics, Chemistry and Dynamics*, ed. G. L. Geernaet, Kluwer, Dordrecht, 327–362.

Arakawa, A. and W. H. Schubert, 1974: Interactions of a cumulus cloud ensemble with the large-scale environment. Part I. *J. Atmos. Sci*., **31**, 674–701.

Bister, M. and K. A. Emanuel, 1998: Disspitative heating and hurricane intensity. *Meteor. Atmos. Phys*., **55**, 233–240.

Chao, W. C., 2000: Multiple quasi equilibria of the ITCZ and the origin of monsoon onset. *J. Atmos. Sci*., **57**, 641–651.

Chen, S.-J., Y.-H. Kuo, W. Wang, Z.-Y. Tao, and B. Cui, 1998: A modeling case study of heavy rainstorms along the Mei-Yu front. *Mon. Wea. Rev*., **126**, 2330–2351.

Detering, H. W. and D. Etling, 1985: Application of the E-ε turbulence model to the atmospheric boundary layer. *Bound.-Layer Meteor*., **33**, 113–133.

Ding, Y.-H., 1993: *Research on the 1991 Persistent, Severe Flood over Yangtze-Huai River Valley*. Chinese Meteor. Press, Beijing, China. ISBN 7-5029-1453-6 (in Chinese).

Dudhia, J., 1989: Numerical study of convection observed during the winter monsoon experiment using a mesoscale two-dimensional model. *J. Atmos. Sci*., **46**, 3077–3107.

Durran, D. R. and J. B. Klemp, 1982: On the effects of moisture on the Brunt-Väisälä frequency. *J. Atmos. Sci*., **39**, 2152–2158.

Edwards, J. M. and A. Slingo, 1996: Studies with a flexible new radiation code. I: choosing a configuration for a large-scale model. *Q. J. R. Meteor. Soc*., **122**, 689–719.

Fairall, C. W., J. D. Kepert and G. J. Holland, 1994: The effect of sea spray on surface energy transports over the ocean. *Global Atmos. Ocean System*, **2**, 121–142.

Fairall, C. W., E. F. Bradley, D. P. Rogers, J. B. Edson, and G. S. Young, 1996: Bulk parameterization of air-sea fluxes for Tropical Ocean-Global Atmosphere Coupled Ocean Atmosphere Response Experiment. *J. Geophys. Res*., **110C**, 3747–3764.

Frank, W. M., 1977: The structure and energetics of the tropical cyclone. I: Storm structure. *Mon. Wea. Rev*., **105**, 1119–1135.

Hess, P. G., D. S. Battisti, and P. J. Rasch, 1993: Maintenance of the intertropical convergence zones and the large-scale tropical circulation on a water-covered earth. *J. Atmos. Sci*., **50**, 691–713.

Heymsfield, A. J. and L. J. Donner, 1990: A scheme for parameterizing ice-cloud water content in

general circulation models. *J. Atmos. Sci*., **47**, 1865–1877.
Holland, G. J., 1995: Scale interaction in the western Pacific monsoon. *Meteor. Atmos. Phys*., **56**, 57–79.
Kang, I.-S., 1999: CLIVAR monsoon modeling intercomparison: Overview. Monsoon Symposium and CLIVAR Monsoon Workshop, Dec. 6–10, 1999, Honolulu, Hawaii.
Krishnamurti, T. N., A. Kumer, K. S. Yap, A. P. Datoor, N. Davidson, and J. Sheng, 1990: Performance of a high-resolution mesoscale tropical prediction model. *Advances in Geophys*., **32**, Academic Press, 133–286.
Kuo, H. L., 1974: Further studies of the parameterization of the influence of cumulus convection on large-scale flow. *J. Atmos. Sci*., **31**, 1231–1240.
Lin, Y.-L., R. D. Farley, and H. D. Orville, 1983: Bulk parameterization of the snow field in a cloud model. *J. Climate Appl. Meteor*., **22**, 1065–1092.
Lindzen, R. S. and A. Y. Hou, 1988: Hadley circulations for zonally averaged heating centered off the equator. *J. Atmos. Sci*., **45**, 2416–2427.
Manabe, S., J. Smagorinsky, and R. F. Strickler, 1965: Simulated climatology of a general circulation model with a hydrological cycle. *Mon. Wea. Rev*., **93**, 769–798.
Molinari, J. and M. Dudeck, 1992: Parameterization of convective precipitation in mesoscale numerical models: A critical review. *Mon. Wea. Rev*., **120**, 326–344.
Numaguti, A. and Y.-Y. Hayashi, 1991: Behaviors of cumulus activity and the structures of circulations in an "aqua planet" model. Part I: The structure of super clusters. *J. Meteor. Soc. Japan*, **69**, 541–561.
Raymond, D. J., 2000: The Hadley circulation as a radiative-convective instability. *J. Atmos. Sci*., **57**, 1286–1297.
Reisner, J., R. M. Rasmussen, and R. T. Bruintjes, 1998: Explicit forecasting of supercooled liquid water in winter storms using MM5 mesoscale model. *Quart. J. Roy. Meteor. Soc*., **124**, 1071–1107.
Rutledge, S. A. and P. V. Hobbs, 1983: The mesoscale and microscale structure and organization of clouds and precipitation in midlatitude cyclones. VIII: A model for the "seeder-feeder" process in warm-frontal rainbands. *J. Atmos. Sci*., **40**, 1185–1206.
Rutledge, S. A. and P. V. Hobbs, 1984: The mesoscale and microscale structure and organization of clouds and precipitation in midlatitude cyclones. XII: A diagnostic modeling study of precipitation development in narrow clod-frontal rainbands. *J. Atmos. Sci*., **41**, 2949–2972.
Sun, Z. and L. Rikus, 1999: Improved application of exponential sum fitting transmissions to inhomogeneous atmosphere. *J. Geophys. Res*., **104**, D6, 6291–6303.
Waliser, D. E. and R. C. J. Somerville, 1994: Preferred latitudes of the intertropical convergence zone. *J. Atmos. Sci*., **51**, 1619–1639.
Wang, B. and Y. Wang, 1999: Dynamics of the ITCZ-equatorial cold tongue complex and causes of the latitudinal climate asymmetry. *J. Climate*, **12**, 1830–1847.
Wang, Y., 1999: A triply-nested movable mesh tropical cyclone model with explicit cloud microphysics. BMRC Research Report, No. 74, Bureau of Meteorology Research Centre. 86 pp.
Wang, Y., 2000: Development of the IPRC Regional Climate Model (RCM) and Modeling of the Asia-Australian Monsoon System (AAMS). A Work Plan submitted to IPRC. 18 pp.
Wang, Y., 2001a: An explicit simulation of tropical cyclones with a triply nested movable mesh primitive equation model-TCM3 Part I: Model description and control experiment. *Mon. Wea. Rev*., **129**, 1370–1394.
Wang, Y., 2001b: Vortex Rossby waves in a numerically simulated tropical cyclone Part I: Overall structure, potential vorticity and energy budgets. *J. Atmos. Sci*. (submitted).
Wang, Y., 2001c: Vortex Rossby waves in a numerically simulated tropical cyclone Part II: The role in tropical cyclone structure and intensity changes. *J. Atmos. Sci*. (submitted).
Zhang, G.-J., 1994: Effects of cumulus convection on the simulated monsoon circulation in a general circulation model. *Mon. Wea. Rev*., **122**, 2022–2038.

Y. Wang (e-mail: yqwang@soest.hawaii.edu) and B. Wang (e-mail: bwang@soest.hawaii.edu)